

Photoemission from single-walled carbon nanotubes

Alireza Nojeh,^{1,a)} Katerina Ioakeimidi,² Samad Sheikhaei,¹ and R. Fabian W. Pease²

¹Department of Electrical and Computer Engineering, University of British Columbia,
2332 Main Mall, Vancouver, BC V6T 1Z4, Canada

²Department of Electrical Engineering, Stanford University, 350 Serra Mall,
Stanford, California 94305, USA

(Received 22 April 2008; accepted 12 June 2008; published online 8 September 2008)

Carbon nanotubes have promising electron emission characteristics. We report on photo-electron emitters made from sparse collections of single-walled carbon nanotubes resting on a silicon dioxide surface. A 266 nm ultraviolet laser was used. The measured emission current suggests a level of optical power absorption of approximately an order of magnitude higher than what is expected purely based on the surface area of the nanotubes; it appears that a more efficient mechanism is at work. We also present simulation results and discuss whether optical antenna effects could provide an insight. © 2008 American Institute of Physics. [DOI: 10.1063/1.2968457]

I. INTRODUCTION

Due to their excellent properties such as outstanding electronic and mechanical characteristics, carbon nanotubes are the subject of intense research for many applications such as quantum dots, transistors, sensors, actuators, and nanocomposites. One particularly promising area has been electron sources for applications ranging from field-emission flat-panel displays¹⁻⁴ to electron-beam systems such as scanning electron microscopes.⁵

Electrons can be emitted from a material (that we refer to as source or emitter) to vacuum in a number of ways. One involves heating the source to a high temperature (typically around 3000 K) so that electrons gain enough kinetic energy to overcome the workfunction barrier. Another method, the so-called field-electron emission (or field-emission for short) relies on the application of a strong external electric field to extract electrons through the quantum-mechanical tunneling process. Fields in the order of several volts per nanometer near the emitter surface are typically necessary. A combination of high temperatures and strong fields leads to the so-called Schottky emission. Another way to assist electrons in overcoming the workfunction barrier is to use light. Thus, in photoelectron emission (photoemission for short), photons with energies higher than the workfunction illuminate the material and cause electron emission (Fig. 1).

Due to the sp^2 carbon-carbon bond, carbon nanotubes have extremely strong mechanical structures. They can pass current densities of several orders of magnitude higher than copper and silver. They show little resistance to the passage of current, and due to the one-dimensional nature of electron transport, they can reach a conductance near the quantum limit. A nanotube with a diameter of only a few nanometers can have a length of up to hundreds of micrometers or even millimeters. This high aspect ratio leads to significant enhancement of an externally applied electric field, making electron emission possible at relatively low applied voltages. Moreover, the one-dimensional nature of nanotubes and the

strong presence of quantum-mechanical effects could lead to properties in nanotube electron sources that are quite different from traditional emitters such as tungsten tips. Nanotube electron sources have been investigated since the early days of nanotube research, with the majority of the activities being on field-emission devices. Reviews on the state of nanotube electron source research can be consulted for more detail.^{6,7} The workfunction of carbon nanotubes is typically in the 4–5.5 eV range. Therefore, relatively high energy photons—ultraviolet (UV) wavelengths or shorter—are necessary for photoemission.

Photoemission spectroscopy has been widely used to study the properties of carbon nanotubes. Fleming *et al.*⁸ studied aligned single-walled carbon nanotubes (SWNTs) on silicon substrates using x-ray absorption and UV photoemission spectroscopy (photon energies of 30 eV and higher). Shiozawa *et al.*⁹ used photoemission spectroscopy to observe peak structures arising from the van Hove singularities in SWNTs. The electronic properties of SWNTs in the presence of donor and acceptor adsorbants were investigated by Larciprete *et al.*¹⁰ Bittencourt *et al.*¹¹ studied the effect of oxygen plasma treatment on the electronic states of multiwalled carbon nanotubes (MWNTs). Ha *et al.*¹² observed significantly delocalized π states in arc discharge-grown nanotubes and investigated their effect in field-electron emission. Recently, Kocharova *et al.*¹³ used photoemission spectroscopy to study nanotube intermolecular interactions and alignment in self-assembled monolayers on gold. In the experiments of Suzuki *et al.*^{14,15} x-ray photoemission microscopy was used to obtain images of SWNTs. Typically photon energies of

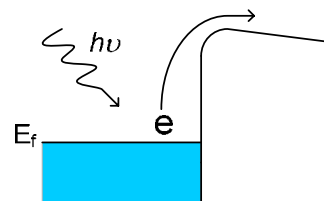


FIG. 1. (Color online) Schematic representation of the photoemission process.

^{a)}Electronic mail: anojeh@ece.ubc.ca.

several tens or hundreds of eV (vacuum UV and soft x-rays) from synchrotron radiation were used in the works above. Another technique in widespread use for the study of nanotube properties is Raman spectroscopy.^{16–20} Suzuki and Kobayashi²¹ used Raman measurements to investigate the damage created in SWNTs by irradiation with photons with energies as low as 20 eV and observed that small-diameter nanotubes are damaged more easily. Recently Kaminska *et al.*²² performed Raman imaging of carbon nanotubes during growth in real time.

The indirect effect of laser irradiation on field-electron emission from nanotubes has also been studied. For example, Rinzler *et al.*²³ observed enhanced emission when the nanotube tips were opened by laser evaporation. Mayer *et al.*²⁴ studied the photon-enhanced field-emission in nanotubes theoretically. The effect of laser pulses on the field-emission of randomly grown mat samples of MWNTs was investigated by Chen *et al.*²⁵ A marked enhancement of the emission current was observed, which the authors attributed to an increase in the effective emission area due to laser heating (given the workfunction of nanotubes, the wavelength of 308 nm used in that experiment, corresponding to a photon energy of 4.03 eV, makes it unlikely that a significant photoemission current was present). Another interesting experiment was recently performed on MWNT films by Wong *et al.*²⁶ They measured electron emission due to laser pulses at three different wavelengths. While they observed photoemission by the 266 nm photons, at 355 and 532 nm they attributed the measured current to thermally assisted field-emission. Hudanski *et al.* recently demonstrated a novel electron source, which combines silicon photodiodes (where light absorption happens) with MWNT field-emitters.²⁷ In this article, we report on direct photoelectron emission from SWNTs, to the best of our knowledge for the first time. Another distinguishing factor between our experiment and the ones discussed above is that our devices consist of a sparse collection of nanotubes rather than a dense collection, with nanotubes far enough from each other that the individual nature of the nanotubes becomes important, as opposed to only a collective behavior. We believe this could play an important role in the effective light absorption properties of each nanotube and the enhanced electron emission currents observed here.

II. DEVICE FABRICATION

Our devices consist of SWNTs lying on a silicon dioxide substrate attached to molybdenum electrodes to enable biasing (Fig. 2). After etching of silicon to create a trench and thermal oxidation to create the dielectric layer (thickness of 1 μm), the electrodes were patterned. SWNTs were then grown from catalyst islands that had been patterned near the edge of the electrodes, using chemical vapor deposition (CVD) with methane and ethylene as carbon source and hydrogen as carrier gas. The catalyst islands consist of iron and molybdenum nanoparticles in an alumina support matrix.²⁸ This particular device structure was chosen due to reasons related to other experiments, beyond the scope of this report. For the experiments described here, all the three electrodes

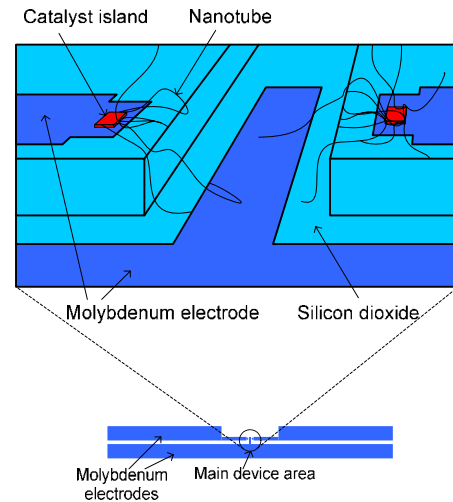


FIG. 2. (Color online) Top: schematic three-dimensional representation of the main device area (width of field of view is 30 μm). Bottom: top view of the large electrode pads that connect to the device in the middle (total electrode length is 9 mm).

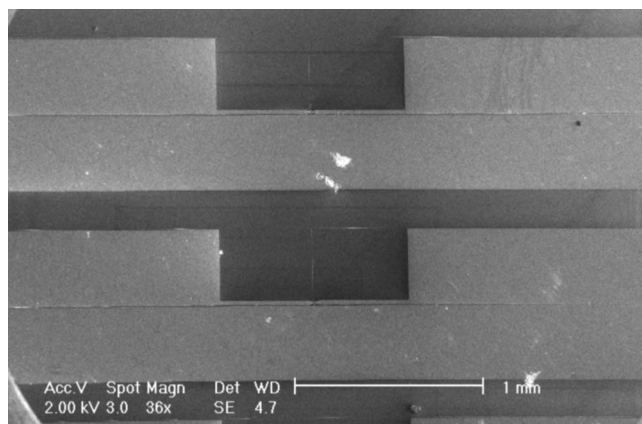
were connected together externally and acted as the cathode in order to ensure the highest level of contact to the nanotubes. The electrodes extend to large pads on both sides that make external contact easy. Figure 3 shows a low-magnification scanning electron micrograph of the side pads with the device area in the middle, together with a high-magnification image of an example device.

III. EXPERIMENTAL APPARATUS

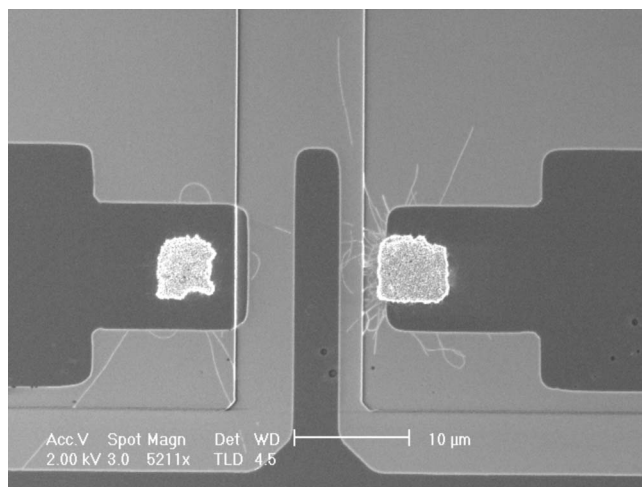
The experiments were performed in a vacuum chamber evacuated to approximately 10^{-5} torr using a turbomolecular pump. A 65 V battery was used to collect the emitted electrons. The collector was placed in the chamber at ~ 5 cm from the device and a sensitive Keithley 485 picoammeter was used to measure the emission current. The laser used was a Coherent, Inc. Azure model, with a wavelength of 266 nm and maximum output power of 200 mW. A window with high UV transmission on the chamber allowed the laser to shine on the sample from one side at a 45° angle. A digital camera was placed in front of another window, looking at the sample at a 45° angle from another side, perpendicular to the laser direction (Fig. 4). The reflection of the laser from the sample surface created a spot that was visualized with the digital camera and allowed us to monitor the precise location of the laser spot. Adjustable mirrors were used to move the laser beam on the sample and illuminate various areas as necessary for the experiments. The diameter of the laser spot on the sample was approximately 1 mm.

IV. RESULTS AND DISCUSSION

In a typical experiment, the laser spot would scan the sample, starting on the large molybdenum pads on one side, passing through the device area (nanotubes), and ending on the far side of the opposite molybdenum pad. The laser power used was 100 mW. The total length of the scan was 9 mm. The measured collector current would thus start at a small value, presumably due to electron emission from the



(a)



(b)

FIG. 3. (a) Low-magnification scanning electron micrograph of the device showing the large metal pads on the side. Two devices can be seen in this figure. (b) High-magnification image of a fabricated device.

molybdenum pad, gradually reach its maximum when the laser was in the middle (over the nanotubes), and then go back to a small value as the laser passed the nanotubes (Fig. 5). The peak in the middle is thus due to the nanotubes.

As mentioned earlier, the laser beam was not highly focused (spot diameter ~ 1 mm). Given the resolution of our laser positioning mechanism, this was essential in order to

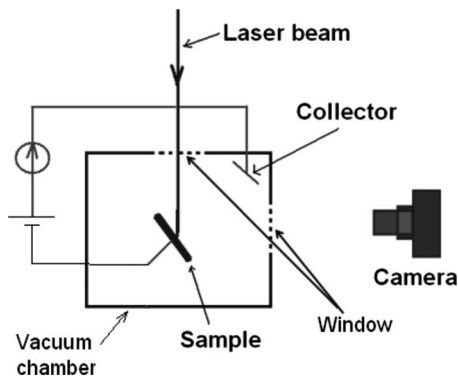


FIG. 4. The diagram of the experimental apparatus.

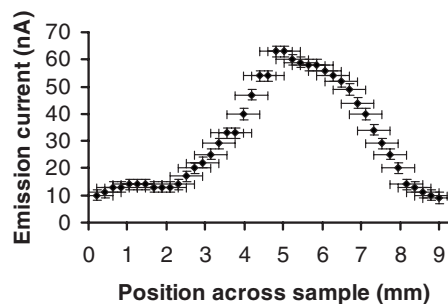


FIG. 5. Emission current vs position of the laser beam on the sample. The device area (nanotubes) is in the middle. The width of the peak is due to the width of the laser spot.

ensure that nanotubes were illuminated at some point during the scan. On the negative side, however, this led to a wide peak in the current versus laser position curve, with its full-width-at-half-maximum determined by twice the laser diameter. Moreover, the large spot size meant correspondingly lower light intensity and therefore less emission current. Nonetheless, clearly there was enough intensity to generate measurable photoemission.

Several important issues need to be considered before attributing the measured current to photoemission from the SWNTs. Since the nanotubes are surrounded by larger structures such as the molybdenum electrodes and catalyst islands, we need to estimate how much of the observed effects are really due to the nanotubes themselves and not the surrounding structures. As can be seen in Fig. 5, obviously there is significantly less emission current when the laser is only illuminating the large molybdenum electrodes (the two far sides of the curve). Therefore it seems reasonable to assume that when the laser is in the middle (over the nanotubes), where the molybdenum electrodes are much smaller than the large side pads, the main contribution to current is not from the electrodes. To further investigate this, we measured the emission current as a function of laser power in two cases, one where the laser spot was positioned on the large molybdenum pads and the other where it was placed in the middle, over the nanotubes. The results clearly indicate higher emission current from nanotubes compared to the molybdenum pads (Fig. 6).

However, one may still argue that the catalyst islands or the exposed silicon dioxide area in the middle [see Fig. 3(b)] can also have a significant contribution to the emission current. In order to test this hypothesis, we repeated the experiment on a sample with molybdenum electrodes and catalyst

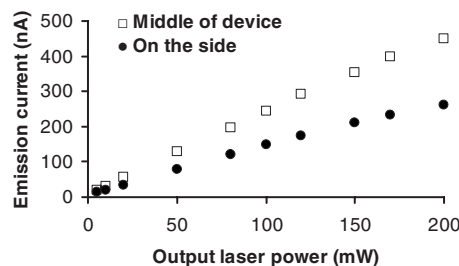


FIG. 6. Emission current vs laser power for two cases: (1) laser spot on the side molybdenum electrode pads (black circles) and (2) laser spot on the nanotubes (empty squares).

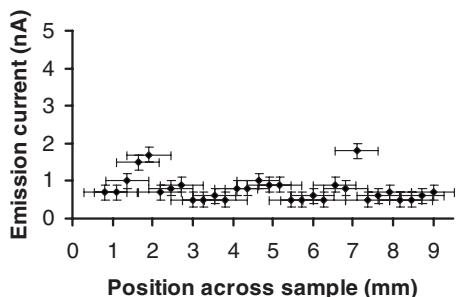


FIG. 7. Emission current vs laser position on a sample with electrodes and catalyst but no nanotube. Clearly, there is no peak in the middle (where catalyst islands and exposed oxide exist), indicating that the catalyst is not a major contributor to the electron emission results shown in Fig. 5.

islands but where no nanotubes had been grown (Fig. 7). As can be seen, there is clearly no maximum in the middle where the catalyst islands are, which leads to the conclusion that the catalyst islands or oxide are not a major contributor to the emission current.

Although the behavior explained so far was somewhat expected, a closer look at the values of the recorded emission current reveals potentially interesting characteristics, drastically different from traditional surface electron emitters. If nanotubes are to act similarly to traditional emitters, the amount of light absorbed could be calculated by knowing the light intensity and the total absorption surface (cross section of the SWNT as seen by the incident light, i.e., diameter \times length). The wavelength of the light was 266 nm, meaning a photon energy of 4.66 eV. Given the incident power level of 100 mW over an area of $\pi \times (0.5 \text{ mm})^2$, this leads to 1.7×10^5 photons/s nm^2 . Even with a quantum efficiency of 100%, this would lead to a 2.7×10^{-14} A of emission current from every nm^2 of the nanotube surface. As can be seen in Fig. 3, the total length of nanotubes in each device is in the range of a few hundred micrometers. Since the average diameter of SWNTs is around 1 nm, this means that each device has an area of a few 10^5 nm^2 covered with nanotubes. This would thus create an emission current of a few nA, which is an order of magnitude below the measured value. It is thus apparent that the estimated absorbed power based on the geometrical surface area of the nanotubes cannot provide a reasonable estimate of the emission current, and a more efficient power absorption mechanism has to be present. Moreover, due to limited collector efficiency and sapphire window transmission in our experiment, as well as the fact that quantum efficiency is much less than 100%, the power absorption coefficient must be even higher than the one order of magnitude suggested by the simple estimate above.

A number of mechanisms could have an effect on the emission current. One possibility is the heating of the oxide surface due to laser irradiation. However, given the thermal conductivity of silicon dioxide (1.1 W/mK) and silicon (>20 W/m K),^{29,30} the oxide thickness of 1 μm , the wafer thickness of 500 μm , and the amount of incident laser power of $1.3 \times 10^5 \text{ W/m}^2$, even if all the energy is absorbed, a simple calculation shows that the temperature of the oxide surface will not rise by more than a few degrees. Therefore, thermionic emission due to substrate heating is ruled out.

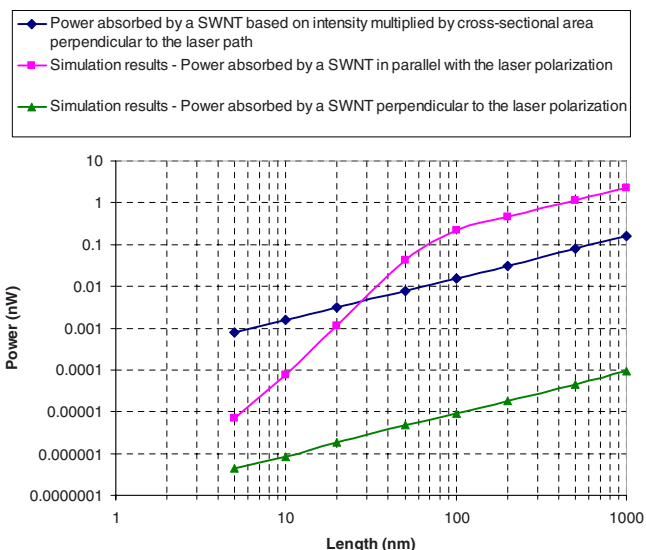


FIG. 8. (Color online) Simulation results for power absorbed by a 1.2 nm diameter SWNT as a function of its length. The nanotube was illuminated by a plane wave with a wavelength of 266 nm.

Another possibility could be efficient energy absorption by nanotubes due to antenna effects, at least in some of the nanotubes with specific lengths. Optical antenna effects in individual or arrays of freestanding nanotubes have been reported previously.^{20,31–33} A number of theoretical works have also been addressing nanotube antennas in frequencies ranging from microwave to the optical regime.^{34–39} However, to the best of our knowledge, there is no previous report of such effects in nanotube photoelectron emitters. We performed classical antenna simulations to investigate this possibility with finite-element analysis using the software COMSOL MULTIPHYSICS. A nanotube was illuminated by a plane wave (wavelength of 266 nm) and the absorbed power measured. The electric field of the incident light was polarized parallel to the nanotube axis. The nanotube was treated as a metallic cylinder with a diameter of 1.2 nm (our CVD-grown nanotubes have a diameter distribution in the 0.7–5 nm range with a peak around 1.2 nm), conductivity of $5 \times 10^7 \text{ S/m}$ (typical of metals such as copper), and a complex permittivity with the real part of $\epsilon_r=60$ and imaginary part of $\epsilon_i=60$. The value of permittivity was chosen based on the argument by Freitag *et al.*⁴⁰ and considering that our incident photons have an energy of 4.66 eV. The simulations were done for various lengths of the nanotube (Fig. 8). The figure also shows the amount of power incident on the geometrical surface area of the nanotube (simply intensity times cross-sectional area perpendicular to the laser path). As the length of the nanotube increases, the absorbed power also increases. However, as can be seen from the results, below a certain critical length the total absorbed power is even less than intensity times nanotube cross section, which hints at inefficient absorption. Beyond this length, the nanotube is acting as an efficient antenna, and absorption is about an order of magnitude higher than intensity multiplied by nanotube cross section and increases linearly with nanotube length. This is in agreement with our experimental measurement of power absorption efficiency (ratio of actual absorbed power to the

value calculated by multiplying intensity and nanotube cross-sectional area perpendicular to the laser path) discussed above. To study the effect of polarization, we also repeated the simulation for the isolated nanotube with the electric field of the incident light perpendicular to the nanotube axis. In this case the absorption is about three orders of magnitude lower than even intensity times surface (Fig. 8). We further studied the effect of polarization, and as expected, the absorbed power has a cosine-type dependence on the angle between the nanotube axis and polarization direction of the electric field (not shown). This all confirms the antenna-like behavior of the nanotubes in this configuration.

In our real devices, most of the nanotubes have lengths of a few micrometers or higher (more than the critical length) and are thus expected to show enhanced absorption as suggested by the simulations. Since their directions are randomly distributed, it is expected that there will always be several nanotubes parallel to the incident field polarization (or at relatively small angles to it), which exhibit enhanced absorption. Unfortunately we do not have experimental data on the effect of polarization at this stage and that will be the subject of future work. The effect of nanotube cross section shape and diameter in our simulations was also studied. It is seen that using a rectangular cross section (as opposed to circular) does not have a significant effect. However, a nanotube with a diameter of 5 nm absorbs about two times more than one with a diameter of 1.2 nm. Therefore, given the diameter distribution in our CVD-grown nanotubes mentioned earlier, some of them could be more efficient in absorbing power than others. All in all, the simulations provide a good justification for enhanced power absorption by the nanotubes.

One important issue to note here is that a portion of the absorbed power is due to the nanotube conductivity. However, this part is in the form of resistive heating and has no direct relation to the photoemission current; care has to be exercised in linking the two. What it suggests is that in a better conductor, the electrons can more easily respond to an applied electromagnetic radiation and create currents oscillating with the same frequency as the illuminating field, leading to the reradiation of a field with that frequency. This extra radiated field effectively enhances the total field felt by some of the other electrons in the nanotube and increases their emission probability. Indeed, in our simulations we observed that the inclusion of conductivity (in addition to the imaginary part of the permittivity) enhances the field amplitude around the tip region by a factor of more than 3, which means an intensity enhancement of about an order of magnitude. Given that electron emission is mainly expected to take place from the nanotube tip region, this could have a significant effect on the emission current. Another important factor to consider is that given the quasi-one-dimensional nature of transport in SWNTs, the electrons are strongly correlated and high-amplitude currents induced in the nanotube (due to its high conductivity) as suggested by the enhanced power absorption might lead to peculiar collective phenomena that effectively enhance electron emission as well. However, at present we do not have any clear explanation for such effects. In other words, although our classical antenna

simulations do provide a justification for the experimental data, it should be noted that more “exotic” phenomena could play an important effect in the efficient conversion of light to emitted electrons observed here. For example, it is known that the localized states near the nanotube tip could play a significant role in field-electron emission.⁴¹ Similar effects might be present here; there could be a strong coupling of light to some of the nanotube tip orbitals, especially given the strong enhancement of the electric field at the nanotube tip. Another possibility to consider is the modulation of the potential barrier (height and slope) by the incident electric field. This could lead to field-emission from the tip during a portion of the cycle when the barrier is narrow enough (the so-called optical field-emission process). Similar effects have been reported by Hommelhoff *et al.*⁴² in photoemission experiments on a tungsten tip. However, this seems unlikely here given that we do not have a strong applied external dc field, and based on our simulations, the electric field of the incident light never reaches the level of several volts per nanometer that is typically needed for field emission. Future work would include the theoretical study of such effects, as well as more controlled experiments on individual SWNTs with various lengths to evaluate any possible antenna effects more quantitatively.

V. CHALLENGES AND DIFFICULTIES

Several challenges and uncertainties are still present in the experiments. The experiments were repeated on a number of samples and devices, and not every device exhibited the same level of electron emission. Obviously, due to the random nature of the nanotube growth process, each device has a unique structure in terms of number, chirality, length, and direction of the nanotubes (although they are predominantly single-walled). This makes it difficult to directly quantify any possible antenna effect referred to earlier. Future work involves a more controlled fabrication of a variety of samples (for example, using electric field assisted growth to obtain aligned nanotubes⁴³) to allow for a more systematic study. Also, the relatively low vacuum of 10^{-5} torr in our chamber could lead to a quick build-up of amorphous carbon on the nanotubes, which would affect their emission properties and create fluctuations in our measurements.⁴⁴ We are working on performing these experiments under high vacuum and ultrahigh vacuum conditions to minimize this effect. The photon energy of 4.66 eV corresponding to the 266 nm wavelength is not high enough to induce photoemission from all nanotubes since some of them can have work-functions of even more than 5 eV. Deeper UV wavelengths could be used to stimulate all the nanotubes.

VI. CONCLUSION

Photoelectron emission from small collections of SWNTs lying on a silicon dioxide surface was studied experimentally using a UV laser. The amount of emission current was significantly higher than what one expects based on the geometrical cross section perpendicular to the laser path. In other words, it appears that the effective absorption cross section of the nanotubes is much higher than their geometri-

cal surface area. Simulations were also performed to investigate this high absorption based on antenna effects at optical frequencies. Other than enhanced light absorption and electron emission that can lead to high-performance electron sources for a variety of applications, these antenna effects could have important implications for carbon nanotube applications in electronics and optoelectronics. As an example, one can imagine a miniaturized telecommunications network where the frequencies in use are optical frequencies and the antennas are made of carbon nanotubes. Potentially some of the current wireless communication techniques could be scaled down in order to create a wireless network on, for instance, an integrated circuit. As one application, this could lead to new solutions to the important interconnect challenge in the semiconductor industry.

ACKNOWLEDGMENTS

We thank Coherent, Inc. for providing the laser on a loan basis, as well as the Stanford Linear Accelerator Center for hosting a part of the experimental work. We also thank Professor Hongjie Dai of the Stanford Chemistry Department for generously providing access to his nanotube growth facility. This work was partially supported by the US Department of the Air Force under Grant No. F33615-00-1-1728, the DARPA ALP, and National Science Foundation NIRT (Grant No. ECS 0210899). Fabrication was performed in part at the Stanford Nanofabrication Facility of NNIN supported by the National Science Foundation under Grant No. ECS-9731293. Support from the Natural Sciences and Engineering Research Council of Canada is also acknowledged.

- ¹W. B. Choi, D. S. Chung, J. H. Kang, H. Y. Kim, Y. W. Jin, I. T. Han, Y. H. Lee, J. E. Jung, N. S. Lee, G. S. Park, and J. M. Kim, *Appl. Phys. Lett.* **75**, 3129 (1999).
- ²S. Yu, S. Jin, W. Yi, J. Kang, T. Jeong, Y. Choi, J. Lee, J. Heo, N. S. Lee, J.-B. Yoo, and J. M. Kim, *Jpn. J. Appl. Phys., Part 1* **40**, 6088 (2001).
- ³W. B. Choi, Y. W. Jin, H. Y. Kim, S. J. Lee, M. J. Yun, J. H. Kang, Y. S. Choi, N. S. Park, N. S. Lee, and J. M. Kim, *Appl. Phys. Lett.* **78**, 1547 (2001).
- ⁴Y.-C. Lan, C.-T. Lee, Y. Hu, S.-H. Chen, C.-C. Lee, B.-Y. Tsui, and T.-L. Lin, *J. Vac. Sci. Technol. B* **22**, 1244 (2004).
- ⁵R. Yabushita, K. Hata, H. Sato, and Y. Saito, *J. Vac. Sci. Technol. B* **25**, 640 (2007).
- ⁶N. de Jonge and J.-M. Bonard, *Philos. Trans. R. Soc. London, Ser. A* **362**, 2239 (2004).
- ⁷P. Yaghoobi and A. Nojeh, *Mod. Phys. Lett. B* **21**, 1807 (2007).
- ⁸L. Fleming, M. D. Ulrich, K. Efimenko, J. Genzer, A. S. Y. Chan, T. E. Madey, S. J. Oh, O. Zhou, and J. E. Rowe, *J. Vac. Sci. Technol. B* **22**, 2000 (2004).
- ⁹H. Shiozawa, H. Ishii, H. Kataura, H. Yoshioka, H. Kihara, Y. Takayama, T. Miyahara, S. Suzuki, Y. Achiba, T. Kodama, M. Nakatake, T. Narimura, M. Higashiguchi, K. Shimada, H. Namatame, and M. Taniguchi, *Physica B (Amsterdam)* **351**, 259 (2004).
- ¹⁰R. Larciprete, A. Goldoni, S. Lizzit, and L. Petaccia, *Appl. Surf. Sci.* **248**, 8 (2005).
- ¹¹C. Bittencourt, A. Felten, B. Dohard, J. Ghijsen, R. L. Johnson, W. Drube, and J. J. Pireaux, *Chem. Phys.* **328**, 385 (2006).

- ¹²B. Ha, J. Park, S. Y. Kim, and C. J. Lee, *J. Phys. Chem. B* **110**, 23742 (2006).
- ¹³N. Kocharova, J. Leiro, J. Lukkari, M. Heinonen, T. Skala, F. Sutara, M. Skoda, and M. Vondracek, *Langmuir* **24**, 3235 (2008).
- ¹⁴S. Suzuki, Y. Watanabe, T. Ogino, Y. Homma, D. Takagi, S. Heun, L. Gregoratti, A. Barinov, and M. Kiskinova, *Carbon* **42**, 559 (2004).
- ¹⁵S. Suzuki, Y. Watanabe, Y. Homma, S. Y. Fukuba, A. Locatelli, and S. Heun, *J. Electron Spectrosc. Relat. Phenom.* **144-147**, 357 (2005).
- ¹⁶H. D. Sun, Z. K. Tang, J. Chen, and G. Li, *Solid State Commun.* **109**, 365 (1999).
- ¹⁷G. S. Duesberg, I. Loa, M. Burghard, K. Syassen, and S. Roth, *Phys. Rev. Lett.* **85**, 5436 (2000).
- ¹⁸A. Jorio, G. Dresselhaus, M. S. Dresselhaus, M. Souza, M. S. S. Dantas, M. A. Pimenta, A. M. Rao, R. Saito, C. Liu, and H. M. Cheng, *Phys. Rev. Lett.* **85**, 2617 (2000).
- ¹⁹A. M. Rao, A. Jorio, M. A. Pimenta, M. S. S. Dantas, R. Saito, G. Dresselhaus, and M. S. Dresselhaus, *Phys. Rev. Lett.* **84**, 1820 (2000).
- ²⁰A. Jorio, A. G. Souza Filho, V. W. Brar, A. K. Swan, M. S. Ünlü, B. B. Goldberg, A. Righi, J. H. Hafner, C. M. Lieber, R. Saito, G. Dresselhaus, and M. S. Dresselhaus, *Phys. Rev. B* **65**, 121402 (2002).
- ²¹S. Suzuki and Y. Kobayashi, *Chem. Phys. Lett.* **430**, 370 (2006).
- ²²K. Kaminska, J. Lefebvre, D. G. Austing, and P. Finnie, *Nanotechnology* **18**, 165707 (2007).
- ²³A. G. Rinzler, J. H. Hafner, P. Nikolaev, L. Lou, S. G. Kim, D. Tomanek, P. Nordlander, D. T. Colbert, and R. E. Smalley, *Science* **269**, 1550 (1995).
- ²⁴A. Mayer, N. M. Miskovsky, and P. H. Cutler, *Phys. Rev. B* **65**, 195416 (2002).
- ²⁵Y.-C. Chen, H.-F. Cheng, Y.-S. Hsieh, and Y.-M. Tsau, *J. Appl. Phys.* **94**, 7739 (2003).
- ²⁶T.-H. Wong, M. C. Gupta, and C. Hernandez-Garcia, *Nanotechnology* **18**, 135705 (2007).
- ²⁷L. Hudanski, E. Minoux, L. Gangloff, K. B. K. Teo, J.-P. Schnell, S. Xavier, J. Robertson, W. I. Milne, D. Pribat, and P. Legagneux, *Nanotechnology* **19**, 105201 (2008).
- ²⁸J. Kong, H. T. Soh, A. M. Cassell, C. F. Quate, and H. Dai, *Nature (London)* **395**, 878 (1998).
- ²⁹See <http://www.memsnet.org/material/silicondioxidesio2film/> for the thermal conductivity of silicon dioxide.
- ³⁰See http://www.efunda.com/materials/elements/TC_Table.cfm?Element_ID=Si for the thermal conductivity of silicon.
- ³¹Y. Wang, K. Kempa, B. Kimball, J. B. Carlson, G. Benham, W. Z. Li, T. Kempa, J. Rybczynski, A. Herczynski, and Z. F. Ren, *Appl. Phys. Lett.* **85**, 2607 (2004).
- ³²J. Rybczynski, K. Kempa, Y. Wang, Z. F. Ren, J. B. Carlson, B. R. Kimball, and G. Benham, *Appl. Phys. Lett.* **88**, 203122 (2006).
- ³³K. Kempa, J. Rybczynski, Z. Huang, K. Gregorczyk, A. Vidan, B. Kimball, J. Carlson, G. Benham, Y. Wang, A. Herczynski, and Z. F. Ren, *Adv. Mater. (Weinheim, Ger.)* **19**, 421 (2007).
- ³⁴P. J. Burke, S. Li, and Z. Yu, *IEEE Trans. Nanotechnol.* **5**, 314 (2006).
- ³⁵G. W. Hanson, *IEEE Trans. Antennas Propag.* **53**, 3426 (2005).
- ³⁶G. W. Hanson, *IEEE Trans. Antennas Propag.* **54**, 76 (2006).
- ³⁷J. Hao and G. W. Hanson, *Phys. Rev. B* **74**, 035119 (2006).
- ³⁸J. Hao and G. W. Hanson, *IEEE Trans. Nanotechnol.* **5**, 766 (2006).
- ³⁹G. Y. Slepian, M. V. Shuba, S. A. Maksimenko, and A. Lakhtakia, *Phys. Rev. B* **73**, 195416 (2006).
- ⁴⁰M. Freitag, Y. Martin, J. A. Misewich, R. Martel, and Ph. Avouris, *Nano Lett.* **3**, 1067 (2003).
- ⁴¹G. Zhou and Y. Kawazoe, *Phys. Rev. B* **65**, 155422 (2002).
- ⁴²P. Hommelhoff, Y. Sortais, A. Aghajani-Talesh, and M. A. Kasevich, *Phys. Rev. Lett.* **96**, 077401 (2006).
- ⁴³A. Ural, Y. Li, and H. Dai, *Appl. Phys. Lett.* **81**, 3464 (2002).
- ⁴⁴A. Nojeh, W.-K. Wong, A. W. Baum, R. F. Pease, and H. Dai, *Appl. Phys. Lett.* **85**, 112 (2004).